RAG-induced DNA lesions activate proapoptotic BIM to suppress lymphomagenesis in p53-deficient mice

Alex R.D. Delbridge,[1,2] Swee Heng Milon Pang,[1,2] Cassandra J. Vandenberg,[1,2] Stephanie Grabow,[1,2] Brandon J. Aubrey,[1,2,3] Lin Tai,[1,2] Marco J. Herold,[1,2] and Andreas Strasser[1,2]

[1]The Walter and Eliza Hall Institute of Medical Research, Parkville, Victoria 3052, Australia
[2]Department of Medical Biology, University of Melbourne, Parkville, Victoria 3010, Australia
[3]Department of Clinical Haematology and Bone Marrow Transplant Service, the Royal Melbourne Hospital, Parkville, Victoria 3050, Australia

Neoplastic transformation is driven by oncogenic lesions that facilitate unrestrained cell expansion and resistance to antiproliferative signals. These oncogenic DNA lesions, acquired through errors in DNA replication, gene recombination, or extrinsically imposed damage, are thought to activate multiple tumor suppressive pathways, particularly apoptotic cell death. DNA damage induces apoptosis through well-described p53-mediated induction of PUMA and NOXA. However, loss of both these mediators (even together with defects in p53-mediated induction of cell cycle arrest and cell senescence) does not recapitulate the tumor susceptibility observed in *p53*$^{-/-}$ mice. Thus, potentially oncogenic DNA lesions are likely to also trigger apoptosis through additional, p53-independent processes. We found that loss of the BH3-only protein BIM accelerated lymphoma development in p53-deficient mice. This process was negated by concomitant loss of RAG1/2-mediated antigen receptor gene rearrangement. This demonstrates that BIM is critical for the induction of apoptosis caused by potentially oncogenic DNA lesions elicited by RAG1/2-induced gene rearrangement. Furthermore, this highlights the role of a BIM-mediated tumor suppressor pathway that acts in parallel to the p53 pathway and remains active even in the absence of wild-type p53 function, suggesting this may be exploited in the treatment of p53-deficient cancers.

INTRODUCTION

Neoplastic transformation, the process leading from a normal cell state into a malignant tumor, is estimated to require at least five to seven oncogenic mutations (Stratton et al., 2009). These oncogenic mutations facilitate unrestrained cell proliferation, evasion from cell death, and escape from immune destruction (Hanahan and Weinberg, 2011). Defects that compromise the ability of cells to detect and repair DNA lesions increase the risk of acquiring oncogenic lesions and thereby predispose to cancer development. Lymphocyte differentiation requires DNA rearrangement at the antigen receptor (*TCR* and *Ig*) gene loci and this is catalyzed by the endonucleases RAG1 and RAG2 (Fugmann et al., 2000). Notably, aberrant RAG1/2 activity can promote tumor development by giving rise to chromosomal translocations that activate oncogenes (e.g., *Myc-Ig*: t[8;14] or *Bcl-2-Ig*: t[14;18]; Marculescu et al., 2002).

To confront the threat posed by acquisition of tumor-promoting mutations, elaborate mechanisms have evolved to ensure that DNA lesions are repaired in a timely manner or, alternatively, that the damaged cell is directed to undergo senescence or cell death to prevent expansion of a nascent neoplastic clone (Lord and Ashworth, 2012). Although apoptosis is recognized as a powerful means to suppress tumor development (Delbridge et al., 2012), it is surprising that no mechanisms have yet been identified by which potentially oncogenic DNA lesions trigger apoptosis to cause extinction of nascent neoplastic cells.

The BCL-2 regulated apoptotic pathway is critical for the initiation of apoptosis in response to many cytotoxic insults, including DNA damage (Czabotar et al., 2014). DNA damage causes activation of p53, which initiates apoptosis through direct transcriptional induction of the proapoptotic BH3-only proteins PUMA and (to a lesser extent) NOXA (Oda et al., 2000; Nakano and Vousden, 2001; Jeffers et al., 2003; Villunger et al., 2003; Yu et al., 2003). However, it has recently been demonstrated that p53 does not suppress tumor development solely through activation of apoptosis (Brady et al., 2011; Li et al., 2012; Valente et al., 2013). In striking contrast to p53-deficient mice, which all succumb to lymphoma (or, more rarely, sarcoma) by ~280 d (Donehower et al., 1992; Jacks et al., 1994), mice lacking all three p53 target genes that are critical for its ability to induce apoptosis (*Puma* and *Noxa*)

Correspondence to Andreas Strasser: strasser@wehi.edu.au; or Alex R.D. Delbridge: alex.delbridge@biogen.com

A.R.D. Delbridge's present address is Neuroimmunology Research, Biogen, Cambridge, MA 02138.

S. Grabow's present address is Dept. of Cancer Immunology and Virology, Dana Farber Cancer Institute, Boston, MA 02115.

Abbreviations used: BH3, BCL2-homology region 3; DN, double negative.

The Rockefeller University Press $30.00
J. Exp. Med. 2016 Vol. 213 No. 10 2039–2048
www.jem.org/cgi/doi/10.1084/jem.20150477

and cell cycle arrest, as well as cell senescence (*p21*), did not develop tumors (Valente et al., 2013). It has therefore been proposed that loss of p53-initiated DNA repair processes underpins the high cancer susceptibility in p53-deficient mice (Valente et al., 2013).

Because DNA damage elicited by chemotherapeutic drugs can induce apoptosis in the absence of p53 (Strasser et al., 1994), it is conceivable that potentially oncogenic DNA lesions (e.g., chromosomal translocations) may also be able to induce apoptosis in a p53-independent manner. It appears likely that BH3-only proteins (activated by DNA lesions in a p53-independent manner) may play a role in such a process (Huang and Strasser, 2000). Accordingly, one would expect that loss of such BH3-only proteins would accelerate tumor development in p53-deficient mice. We report that loss of BIM, but not loss of BMF, collaborates potently with loss of p53 in lymphomagenesis. Interestingly, this acceleration in lymphoma development exerted by loss of BIM could be prevented by concomitant loss of RAG1. These results reveal that BIM-dependent apoptosis is a critical tumor suppressive process activated by RAG1/2-induced DNA lesions.

RESULTS

Loss of BIM, but not loss of BMF, cooperates with loss of p53 to promote tumor development

BIM and BMF are proapoptotic BH3-only members of the BCL-2 family and both have been implicated in DNA damage–induced apoptosis. Because they can both be activated by DNA damage in a p53-independent manner (Bouillet et al., 1999; Labi et al., 2008; Kelly et al., 2010), we examined the impact of their loss on tumor development in p53-deficient mice. We thereby sought to determine whether loss of apoptosis induced by either BIM or BMF would synergize with loss of p53-initiated DNA repair signaling (and potentially loss of other p53-activated tumor suppressive processes), resulting in accelerated tumor development. Accordingly, mice deficient for both p53 and BMF or p53 and BIM were generated and aged to determine their rates of tumor development.

Loss of BMF had no discernible impact on the incidence or rate of tumor development, the type of cancer that developed, and the severity of malignant disease in both $p53^{+/-}$ and $p53^{-/-}$ mice (Fig. 1 and not depicted). In contrast, loss of BIM provoked a substantial acceleration in the already rapid rate of tumor development that is caused by complete loss of p53 (Fig. 2 A; $P < 0.0001$). Strikingly, loss of even a single *Bim* allele was sufficient to accelerate tumor development in $p53^{-/-}$ mice (Fig. 2 A; $P = 0.028$). Loss of BIM also significantly augmented lymphoma burden in the thymus of sick mice (Fig. 2 B), the primary site of tumor growth in $p53^{-/-}$ mice (Donehower et al., 1992; Jacks et al., 1994).

Analysis of aged $Bim^{-/-}$ mice revealed evidence of neoplastic growth, consistent with a previous study (Erlacher et al., 2006), providing evidence for the importance of BIM in tumor suppression. Serum analysis revealed the presence of paraproteins in 8/21 $Bim^{-/-}$ mice at 4–9 mo of age (median age: 7 mo); this is indicative of abnormal neoplastic expansion of a plasma cell clone (Davidson et al., 1998). Moreover, histological examination revealed abnormal infiltration of lymphoid cells into the lungs and kidneys of aged $Bim^{-/-}$ mice (Fig. 2 C). Spleen cells from three aged $Bim^{-/-}$ mice were injected into two RAG1-deficient recipient mice and two wild-type recipient mice each. Interestingly, tumor growth was observed in 4/6 RAG1-deficient recipients but in none of the wild-type recipients. Thus, we conclude that loss of BIM is sufficient to allow cells to become partially transformed with additional oncogenic lesions required for complete escape from host tumor suppression.

To investigate the importance of BIM in a clinically relevant context, mice heterozygous for *p53* (a model of Li Fraumeni syndrome) and also deficient for *Bim* were generated. Loss of BIM markedly accelerated tumor development in $p53^{+/-}$ mice (Fig. 3 A; $P = 0.014$). In particular, loss of BIM substantially increased the incidence of lymphoma in $p53^{+/-}$ mice. Consistent with published results (Donehower et al., 1992; Jacks et al., 1994), the few $p53^{+/-}$ mice that developed tumors presented mostly with sarcoma (three out of four sick mice by 450 d). In contrast, the majority of sick $p53^{+/-}Bim^{-/-}$ (13/15) and $p53^{+/-}Bim^{+/-}$ mice (16/21) presented with lymphoma, commonly of thymic origin (Fig. 3 B).

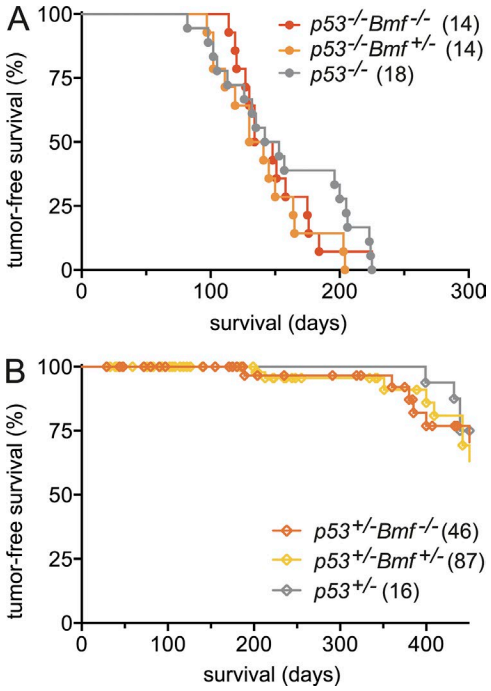

Figure 1. **Loss of BMF does not enhance tumor development in p53-deficient mice.** Kaplan-Meier survival analysis of (A) $p53^{-/-}$ mice or (B) $p53^{+/-}$ mice lacking one of both alleles of *Bmf*. Mouse numbers (*n*) for each genotype are indicated; $p53^{-/-}$ (18), $p53^{-/-}Bmf^{+/-}$ (14), $p53^{-/-}Bmf^{-/-}$ (14), $p53^{+/-}$ (16), $p53^{+/-}Bmf^{+/-}$ (87), and $p53^{+/-}Bmf^{-/-}$ (46). No statistically significant differences in the rate of tumor onset were observed (Kaplan-Meier, log-rank Mantel-Cox test).

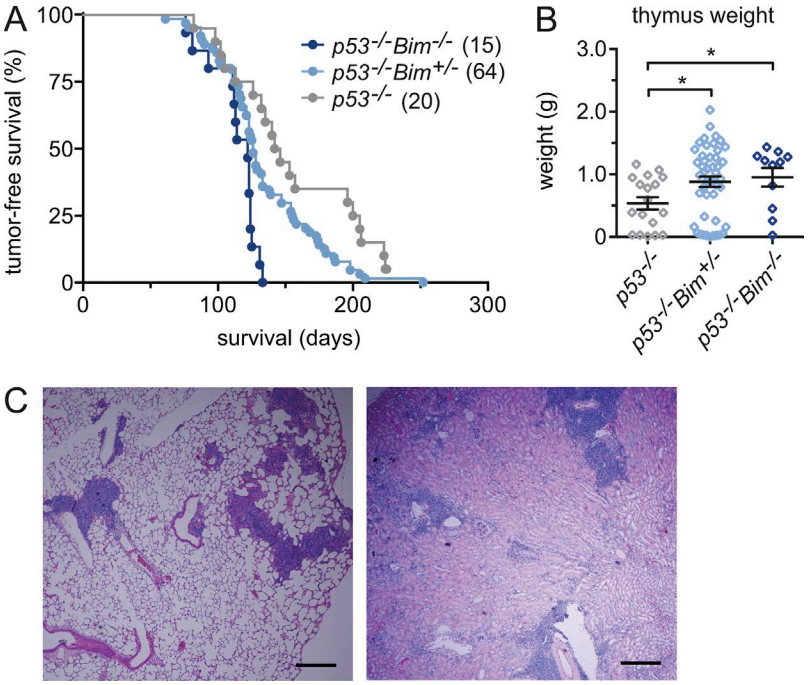

Figure 2. **Loss of BIM enhances lymphoma development in p53-deficient mice.** (A) Kaplan-Meier survival analysis of $p53^{-/-}$ mice compared with $p53^{-/-}$ mice also lacking one or both alleles of *Bim*; median survival in days: $p53^{-/-}$ 144, $p53^{-/-}Bim^{+/-}$ 126, and $p53^{-/-}Bim^{-/-}$ 122. $p53^{-/-}Bim^{-/-}$ versus $p53^{-/-}$, $P < 0.0001$; $p53^{-/-}Bim^{+/-}$ versus $p53^{-/-}$, $P = 0.028$ (Kaplan-Meier, log-rank Mantel-Cox test). (B) Analysis of lymphoma burden in sick mice from A. Mouse numbers for each genotype are indicated; $n = 15–64$. Data are presented as mean ± SEM. *, $P < 0.05$ (Student's *t* test, unpaired two-tailed). (C) Lung (left) and kidney (right) sections from a $Bim^{-/-}$ mouse aged 276 d. Bars, 200 µm.

To determine whether loss of BIM altered the frequency of loss of the remaining wild-type p53 allele (loss of heterozygosity) in the tumors that arise in $p53^{+/-}$ mice, we tested malignant cells harvested from $p53^{+/-}Bim^{-/-}$ mice for markers of p53 pathway activity. p53 pathway activity was abrogated in four of the eight tumors analyzed, as indicated by overexpression of p19 (Fig. 3 C), which is maintained at low levels in the presence of functional p53 (Eischen et al., 1999). DNA sequencing of the *p53* locus in the four of eight tumors that had retained functional p53 signaling revealed, as expected, no evidence for p53 mutations. These findings are consistent with a previous study, which showed that ∼50% of tumors from $p53^{+/-}$ mice (<18 mo of age) had retained the wild-type *p53* allele (Venkatachalam et al., 1998).

RAG1/2 activity is required for the ability of loss of BIM to accelerate lymphoma development in p53-deficient mice

RAG and TdT activities, which during lymphocyte differentiation are essential for antigen receptor gene rearrangement and nucleotide sequence diversification at the junctions, are known sources of oncogenic mutations (e.g., chromosomal translocations; Alt et al., 2013). Accordingly, loss of the activity of the DNA ligases that are critical for the fusion of gene segments during TCR and BCR gene rearrangement substantially accelerates lymphoma development in $p53^{-/-}$ mice (Frank et al.,

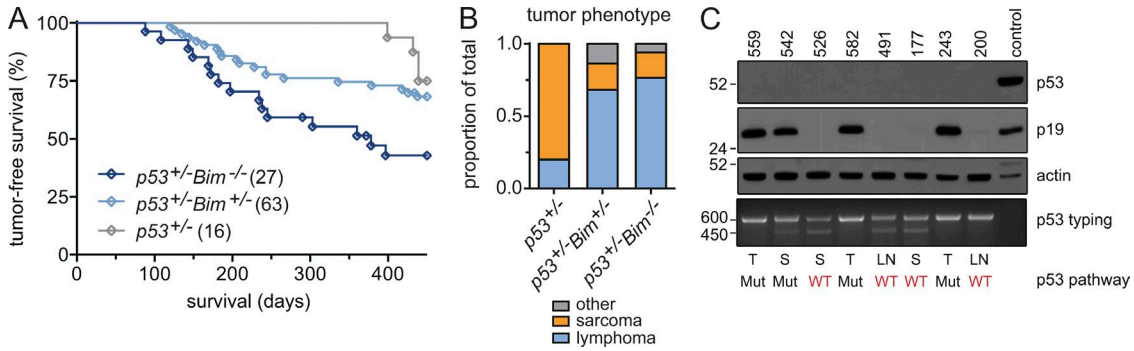

Figure 3. **Loss of BIM enhances lymphoma development in $p53^{+/-}$ heterozygous mice.** (A) Kaplan-Meier survival analysis of $p53^{+/-}$ mice compared with $p53^{+/-}$ mice also lacking one or both alleles of *Bim*. Percentages of mice alive at endpoint (450 d): $p53^{+/-}$, 75%; $p53^{+/-}Bim^{+/-}$, 68%; and $p53^{+/-}Bim^{-/-}$, 43%. $p53^{+/-}Bim^{-/-}$ versus $p53^{+/-}$, $P = 0.0142$; $p53^{+/-}Bim^{+/-}$ versus $p53^{+/-}$, $P = 0.439$. (B) Analysis of tumor phenotype of the sick mice from A. (C) Western blot and *p53* gene sequencing analysis of a subset of tumors from $p53^{+/-}Bim^{-/-}$ mice depicted in A. Red denotes samples that were confirmed wild-type *p53* by gene sequencing. Source of sample analyzed is indicated as follows: spleen (S), thymus (T), lymph node (LN). Mouse numbers (*n*) for each genotype are indicated; $n = 16–63$ (A and B) and 8 (C). Size markers in C are in kilodaltons for Western blots and in base pairs for PCR genotyping.

2000; Gao et al., 2000). We wondered whether BIM might be critical for the induction of apoptosis that can be triggered in response to potentially oncogenic DNA lesions that can arise from the RAG1/2 and TdT activities. This hypothesis was tested by generating chimeric mice with a hematopoietic system deficient for *p53*, *Bim* and *Rag1* ($p53^{-/-}Bim^{-/-}Rag1^{-/-}$), and appropriate controls (i.e., mice with a $p53^{-/-}Bim^{-/-}$, $p53^{-/-}Rag1^{-/-}$ or a $p53^{-/-}$ hematopoietic system). Consistent with our analysis of mice lacking both p53 and BIM in all tissues (Fig. 2), combined loss of p53, and BIM only in hematopoietic cells provoked lymphoma development significantly faster than loss of p53 alone (Fig. 4; $P < 0.0001$). Remarkably, this acceleration in tumor development was abrogated by additional loss of RAG1, increasing median tumor-free survival from 111 d ($p53^{-/-}Bim^{-/-}$) to 168 d ($p53^{-/-}Bim^{-/-}Rag1^{-/-}$; $P < 0.0001$), which is comparable to mice with a $p53^{-/-}Rag1^{-/-}$ (165 d) or a $p53^{-/-}$ hematopoietic system (196 d).

Interestingly, combined loss of RAG1 and BIM resulted in an altered tumor spectrum on a p53-deficient background, with an increased proportion of pro–B/pre–B cell lymphomas, a tumor type that is only rarely observed in mice with either a $p53^{-/-}Bim^{-/-}$ or a $p53^{-/-}$ hematopoietic system, at least on a C57BL/6 background (Fig. 5 A). The reason for this is not clear, but the finding may indicate that in the absence of RAG1/2 activity, pro–B cells may be more genomically unstable than pro–T cells. The former would therefore be more prone to acquiring oncogenic lesions that drive lymphomagenesis.

Tumor burden at autopsy was comparable between mice of the different genotypes with the exception of increased tumor burden in the thymus of the $p53^{-/-}Bim^{-/-}$ hematopoietic chimeric mice (Fig. 5 B), similar to what we observed in the germline *p53* plus *Bim*-deleted animals (Fig. 2 B).

These results demonstrate that RAG1/2 DNA recombination activity is required for the ability of loss of BIM to accelerate lymphoma development in p53-deficient mice.

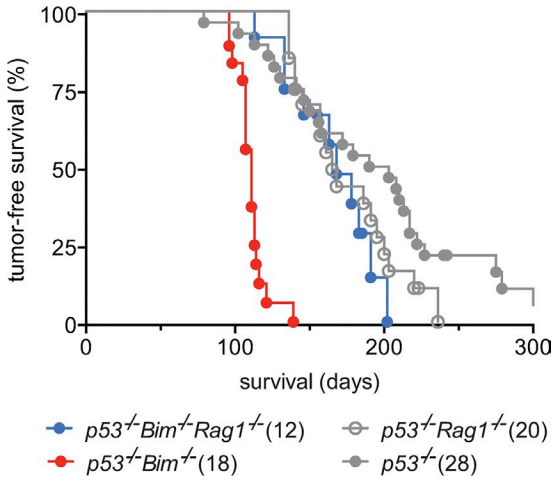

Figure 4. **RAG1 is essential for the acceleration of lymphoma development in p53-deficient mice caused by loss of BIM.** Kaplan-Meier survival analysis of mice with a $p53^{-/-}Bim^{-/-}Rag1^{-/-}$, $p53^{-/-}Bim^{-/-}$, $p53^{-/-}Rag1^{-/-}$, or $p53^{-/-}$ hematopoietic system. Median survival in days: $p53^{-/-}Bim^{-/-}Rag1^{-/-}$, 168; $p53^{-/-}Bim^{-/-}$, 111; $p53^{-/-}Rag1^{-/-}$, 165; and $p53^{-/-}$, 196. $p53^{-/-}Bim^{-/-}Rag1^{-/-}$ versus $p53^{-/-}Bim^{-/-}$, $P < 0.0001$; $p53^{-/-}Bim^{-/-}$ versus $p53^{-/-}$, $P < 0.0001$. Mouse numbers (*n*) for each genotype are indicated in brackets; $n = 12–28$.

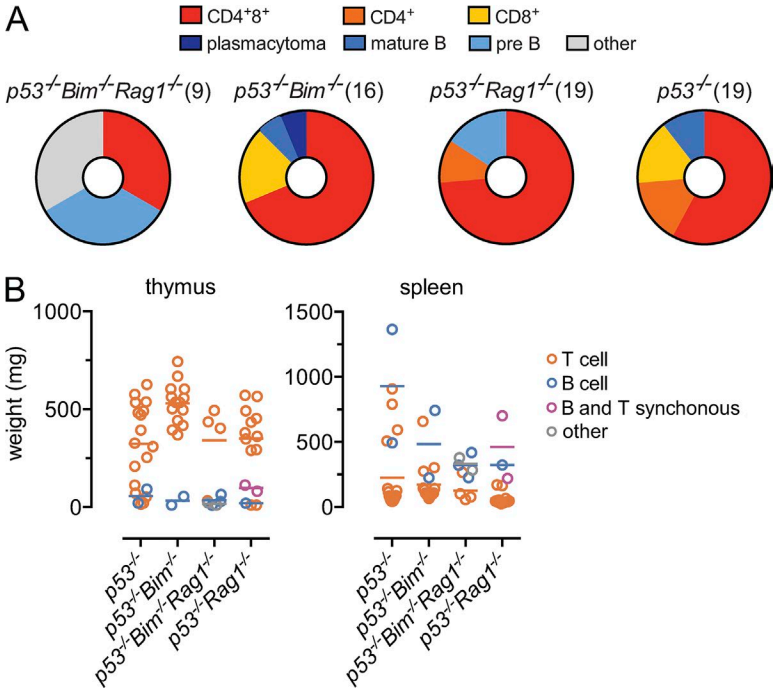

Figure 5. **In the absence of RAG1, loss of BIM promotes pre–B cell lymphoma development in p53-deficient mice.** (A) Immunophenotyping of the tumors from sick mice bearing a $p53^{-/-}Bim^{-/-}Rag1^{-/-}$, $p53^{-/-}Bim^{-/-}$, $p53^{-/-}Rag1^{-/-}$, or $p53^{-/-}$ hematopoietic system. (B) Tumor burden of the sick mice in A. Mouse numbers (*n*) for each genotype are indicated in brackets in A or by individual symbols in B; $n = 9–19$. Bars in B indicate mean values for each tumor subtype.

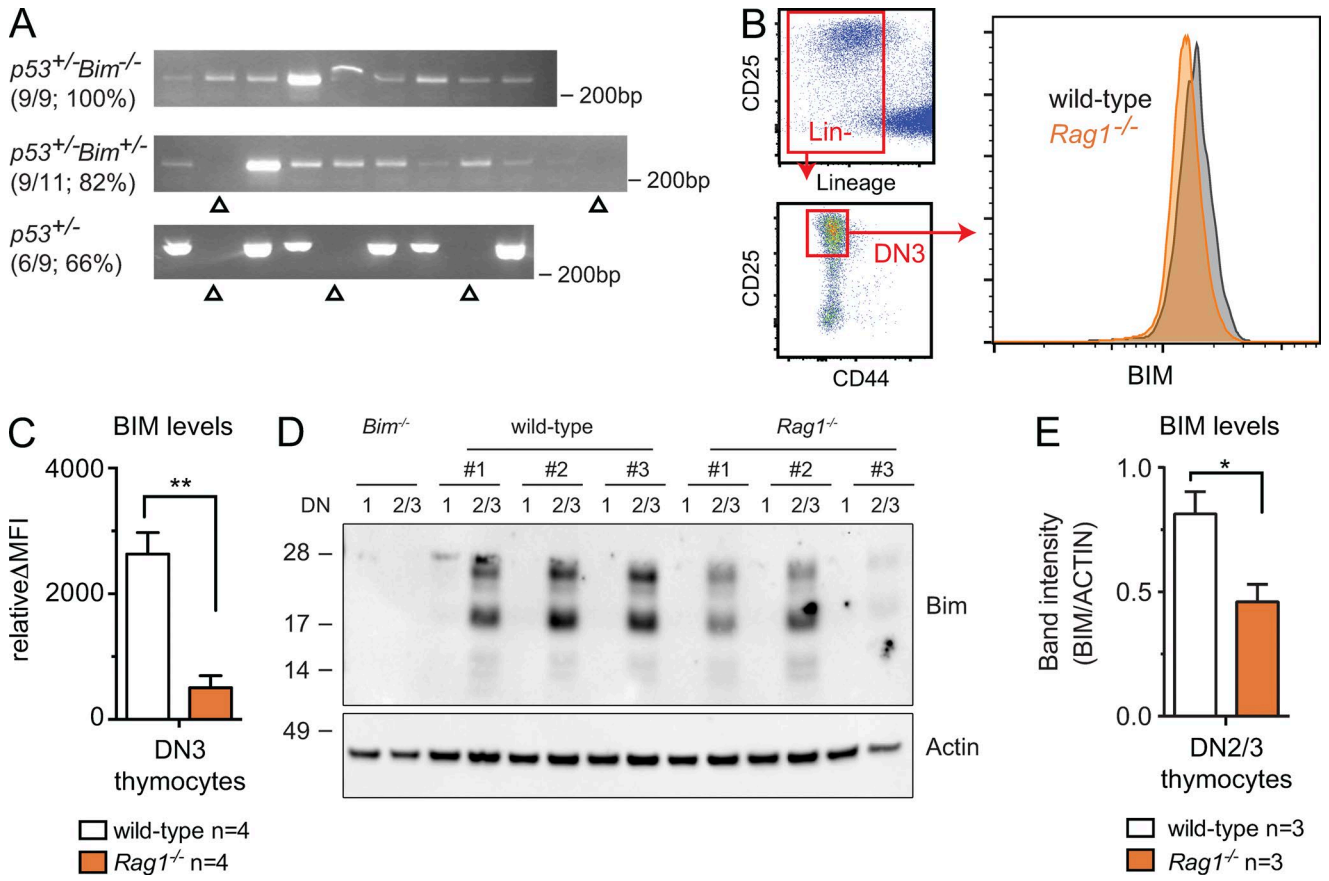

Figure 6. **RAG1 DNA recombinase activity increases the levels of BIM in T cell progenitors.** (A) Tumor samples isolated from $p53^{+/-}Bim^{-/-}$, $p53^{+/-}Bim^{+/-}$, and $p53^{+/-}$ mice were analyzed by PCR to determine the frequency of productive TCRβ gene segment rearrangements; each lane represents an independent lymphoma. Triangles denote tumors with failed TCRβ gene rearrangement (D-J segment ligation). n = 9–11. (B and C) Intracellular FACS analysis was performed on $Lin^-CD25^+CD44^-$ (DN3) thymocytes from $Rag1^{-/-}$ and wild-type mice to determine the levels of BIM protein. In B, representative samples of surface and intra-cellularly stained cells are shown and quantitated results are presented in C. n = 4/genotype; relative ΔMFI represents the signal above background (corresponding cells from $Bim^{-/-}$ mice; i.e., negative control) relative to the signal in DN3 thymocytes from the $Rag1^{-/-}$ mice. (D) Western blot analysis of FACS-sorted in vitro–differentiated T cell progenitors from the indicated stages. Each sample is independent and corresponds to cells differentiated from pooled HSPCs from two mice of the indicated genotypes (n = 3 pooled samples). (E) Quantitation by densitometry of the Western blot data presented in D. Data are presented as mean ± SEM. *, P = 0.0362 (Student's t test, unpaired two-tailed); **, P = 0.0016.

RAG1/2 induced DNA lesions increase the levels of the proapoptotic BH3-only protein BIM

The ability of RAG1 deficiency to abrogate the synergy between loss of BIM and loss of p53 in lymphomagenesis suggests that aberrant RAG1/2 activity may be present in $p53^{-/-}Bim^{-/-}$ lymphoma-initiating cells and, by extension, also in the resulting lymphomas. To search for evidence of aberrant RAG1/2 activity in the $p53^{-/-}Bim^{-/-}$ tumors, we performed PCR analysis to discriminate between productive and nonproductive D-J TCRβ chain gene segment rearrangements, using published methods (Zhang et al., 2011). Productive TCRβ chain gene rearrangements were found in 9/9 $p53^{+/-}Bim^{-/-}$ tumors, but only in 9/11 $p53^{+/-}Bim^{+/-}$ lymphomas and 6/9 $p53^{+/-}$ lymphomas (Fig. 6 A). This indicates that the absence of BIM may facilitate prolonged RAG1/2 activity in T cell progenitors, and thereby allow a higher rate of RAG1/2-induced productive recombination events.

We next wondered whether DNA lesions emanating from *TCR* or *Ig* gene rearrangement might cause an increase in BIM levels in lymphoid progenitors. To investigate this, we performed intracellular FACS analysis to compare the levels of BIM protein in $Lin^-CD25^+CD44^-$ (DN3) T cell progenitors between wild-type and $Rag1^{-/-}$ (no antigen receptor gene rearrangement possible) mice (Fig. 6, B and C). Consistent with our hypothesis, we observed higher BIM levels in wild-type DN3 cells compared with those lacking RAG1. To confirm these findings using an orthogonal approach, we sorted bone marrow progenitor cells from wild-type, $Rag1^{-/-}$ and $Bim^{-/-}$ (negative control for BIM protein detection) mice and performed in vitro differentiation on OP9-DL1 stromal cells (Carotta et al., 2011). Populations of DN1 cells

($Lin^-cKIT^+CD25^-$) and DN2/3 cells ($Lin^-cKIT^{+/-}CD25^+$) were isolated by cell sorting. Western blot analysis revealed elevated BIM protein levels in the wild-type DN2/3 cells compared with the *Rag1*$^{-/-}$ DN2/3 cells (Fig. 6, D and E). No BIM was observed in the DN1 cells of any genotype.

Collectively, these results indicate that loss of BIM may allow the survival of p53-deficient lymphoma-initiating cells with RAG1/2 induced (potentially oncogenic) DNA lesions, thereby fostering neoplastic transformation to malignancy. They also suggest that after select DNA damaging events, BIM is induced and activates apoptosis to enforce tumor suppression, even in the absence of p53.

DISCUSSION

BIM is a potent tumor suppressor in a MYC-driven mouse lymphoma model (Egle et al., 2004), and the *BIM* gene is lost or silenced in several human cancers, including mantle cell lymphoma or renal cancer (Tagawa et al., 2005; Sturm et al., 2006; Mestre-Escorihuela et al., 2007; Zantl et al., 2007; Greenhough et al., 2010; Richter-Larrea et al., 2010). A previous study using a low-dose γ-irradiation–induced lymphoma model in p53-deficient mice has highlighted the contribution of genetic factors in addition to p53 in the suppression of hematopoietic tumor development (Kemp et al., 1994). Our data shed new light on the mechanisms by which BIM suppresses tumor development and reveal how apoptosis can be activated by potentially oncogenic DNA lesions in a p53-independent manner to eliminate nascent cancer-initiating cells. Specifically, we show that loss of BIM accelerates lymphoma development in *p53*$^{-/-}$ and even *p53*$^{+/-}$ heterozygous mice. We also show that RAG1/2 gene rearrangement activity is required for the synergy between loss of BIM and loss of p53 in lymphomagenesis. Thus, we conclude that BIM is activated in response to DNA lesions caused by RAG1/2 DNA recombination activity to eliminate nascent cancer-initiating cells harboring potentially oncogenic DNA lesions.

Previous studies have demonstrated normal thymic cellularity in *Bim*$^{-/-}$ mice, albeit with abnormally increased numbers of mature T cells and reduced immature $CD4^+CD8^+$ thymocytes (Bouillet et al., 1999; Pellegrini et al., 2003; Erlacher et al., 2006). These mice also have normal (or even enhanced) immune function (Pellegrini et al., 2003). Thus, it appears unlikely that impaired antitumor immunity contributes to the acceleration in tumor development caused by loss of BIM on a p53-deficient background.

Although the study presented here focuses predominantly on T lineage lymphomas, sustained survival of lymphoid progenitors with RAG1/2 activity permitted by loss of BIM is likely to also promote development of B lineage lymphomas. Loss of BIM is found in ∼15% of human mantel cell lymphoma cases (Tagawa et al., 2005), and loss of BIM enhances tumor development in a mouse model of this malignancy, which is driven by transgenic cyclin D1 overexpression (Katz et al., 2014). Given that BIM's critical role as an inducer of apoptosis is most evident in lymphoid and myeloid cells (Delbridge and Strasser, 2015), it appears likely that our findings will be of most relevance to hematological cancers. This tissue-predominant function of BIM probably also underpins the selective effect of its loss in enhancing the development of lymphoma in *p53*$^{+/-}$ mice, resulting in increased lymphoma incidence (with concomitantly reduced sarcoma incidence).

The molecular mechanisms that activate BIM in response to DNA lesions, including those caused by aberrant RAG1/2 activity, are unknown. Indeed, recent studies have further highlighted the absence of mechanistic insight into how BIM is activated by cell death stimuli more generally (Clybouw et al., 2012; Herold et al., 2013), questioning previous studies that found transcriptional regulation by FOXO3a (Dijkers et al., 2000) or direct phosphorylation by ERK (Ley et al., 2004) to be critical. The mechanisms that control BIM expression therefore remains a topic of high interest to the field of cell death research. In light of the data presented here, it is interesting to speculate that pathway components upstream of BIM may be disrupted in those cases of mantel cell lymphoma that retain wild-type *BIM*.

MATERIALS AND METHODS

Mice

Experiments with mice were conducted according to the guidelines and with approval from the Walter and Eliza Hall (Parkville, Victoria, Australia) Institute Animal Ethics Committee. *p53*$^{-/-}$ (Jacks et al., 1994), *Bim*$^{-/-}$ (Bouillet et al., 1999), *Bmf*$^{-/-}$ (Labi et al., 2008), and *Rag1*$^{-/-}$ (Mombaerts et al., 1992) mice have been previously described. All strains, except the *Bmf*$^{-/-}$ mice, were originally generated on a mixed C57BL/6 × 129SV background using 129SV-derived ES cells and were backcrossed to C57BL/6 mice for >20 generation before the current study. The *Bmf*$^{-/-}$ mice were generated on an inbred C57BL/6 background using C57BL/6-derived ES cells, and the *Bmf*$^{-/-}$ mice were maintained on this background. Compound mutant mice were generated by intercrossing the relevant single-knockout strains. Genotyping protocols will be made available on request. This study was aided by gifts of mice from the following investigators: T. Jacks (Koch Institute for Integrative Cancer Research at MIT, Boston, MA), A. Villunger (Medizinische Universität Innsbruck, Innsburck, Austria), J. Adams (Walter and Eliza Hall Institute of Medical Research [WEHI], Parksville, Victoria, Australia), S. Cory (WEHI), L. Corcoran (WEHI), C. Scott (WEHI), and P. Bouillet (WEHI).

Chimeric mice reconstituted with the hematopoietic system of compound mutant mice and controls were generated through timed matings of mice lacking various combinations of *p53*, *Rag1*, and *Bim*. Fetal liver cells were isolated from embryonic day 13 embryos and used to reconstitute four lethally irradiated (2 × 5.5 Gy, 3 h apart) C57BL/6-Ly5.1 mice. Recipient mice were maintained on neomycin sulfate–supplemented (Sigma-Aldrich) drinking water for 21 d after γ-irradiation to prevent infection. Such reconstituted mice were monitored thrice weekly for signs

of lymphoma development (lymphadenopathy, splenomegaly, and respiratory difficulties).

Analysis of lymphoma-bearing mice

Immediately before sacrifice, peripheral blood was obtained by retroorbital bleed and collected into heparinized tubes. Total white blood cell, red blood cell, and platelet numbers were determined in an Advia 120 machine using the mouse analysis software module (Bayer). At autopsy, the weights of the spleen, thymus, and lymph nodes (inguinal, axillary, and brachial) of sick mice were determined and the major organs were collected for histological analysis. Mice were deemed to be lymphoma bearing based on abnormal enlargement of the lymphoid organs, elevated peripheral blood counts, infiltration of tumor cells into nonlymphoid organs (such as the liver, lungs, and kidneys), and by abnormal cell surface marker expression. In the case of chimeric (hematopoietic system reconstituted) mice, lymphoma cells were verified to be of donor origin based on expression of Ly5.2. Ambiguity on whether a mouse indeed had a lymphoma was resolved through transplantation and/or tissue culture to determine whether lymphoma cell lines could be established in vivo and/or in vitro. Sarcomas were identified on the basis of characteristic presentation at autopsy and by histological analysis.

Genomic analysis of tumors

Retention versus loss of the wild-type *p53* allele was examined by PCR; primers and PCR conditions will be made available on request. D-J β-chain TCR gene segment ligation efficiency was investigated by PCR using previously published methods (Zhang et al., 2011).

Sequencing of genomic DNA was performed on coding regions of the *Trp53* gene from exon 4–10 inclusive, encompassing the entire DNA-binding domain. Sequencing was performed using the Illumina MiSEQ platform as previously described (Aubrey et al., 2015). Primer sequences were designed to target intron genomic DNA sequence flanking each exon as follows: exon 4–1 for-5′-CAGAGC AGAAAGGGACTTGG-3′ and rev-5′-CGCCATAGT TGCCCTGGTAAG-3′; exon 4–2 for-5′-TTTTGAAGG CCCAAGTGAAG-3′ and rev-5′-AGGCATTGAAAG GTCACACG-3′; exon 5 for-5′-CGACCTCCGTTCTCT CTCC-3′ and rev-5′-GAGGCTGCCAGTCCTAACC-3′; exon 6 for-5′-CGGCTTCTGACTTATTCTTGC-3′ and rev-5′-CCCTTCTCCCAGAGACTGC-3′; exon 7 for-5′-GTAGGGAGCGACTTCACCTG-3′ and rev-5′-CCC TAAGCCCAAGAGGAAAC-3′; exon 8 for-5′-TCTTAC TGCCTTGTGCTGGTC-3′ and rev-5′-TGTGGAAGG AGAGAGCAAGA-3′; exon 9 for-5′-CCCAAAGTCACC TCTTGCTC-3′ and rev-5′-GAGAACCACTGTCGG AGGAG-3′; and exon 10 for-5′-GGTTGTGTGACCTTG TCCAG-3′ and rev-5′-AGCAGGGTGGGGTTTTTATC-3′. Each primer set was made to include a nested sequence for secondary amplification and indexing as previously described (Aubrey et al., 2015).

T cell progenitor in vitro differentiation

To isolate hematopoietic progenitors, femurs, and tibias were isolated, and flushed into balanced salt solution (BSS; Thermo Fisher Scientific). Isolated cells from two mice were pooled into a single sample. The cell suspensions were later prepared in BSS supplemented with 2% (vol/vol) fetal calf serum. Antibodies to the following surface molecules were used as supernatants for immune-magnetic bead depletion of lineage $(Lin)^+$ BM cells: CD3 (KT3-3.1), CD8 (53–6.7), CD2 (RM2-1), B220 (RA3-6B2), MAC-1 (M1-70), GR-1 (RB6-8C5), and erythrocyte (TER119). Cell suspensions were mixed with BioMag goat anti–rat IgG antibody-coupled beads (QIAGEN), and depleted of Lin^+ cells with a Dynal MPC-L magnetic particle concentrator (Invitrogen). Lin^- BM cells were then stained using fluorescently conjugated antibodies as described: goat anti–rat IgG (H+L) antibodies conjugated to Alexa Fluor 680 (Invitrogen), c-Kit APC (2B8), SCA-1 PECy7 (E13161.7), and CD25 Pacific Blue (PC61). Cells were stained for 20–30 min on ice with fluorescently conjugated antibodies, and sorted on FACSAria II (BD) for LSK (Lin^- SCA-1^+ c-KIT^+) cells. Dead cells were excluded by staining with propidium iodide (PI; 2 μg/ml).

The sorted cells were seeded on OP9-DL1 stromal cells in the presence of 100 ng/ml stem cell factor (SCF), 5 ng/ml FLT3L, and 2% IL-7 supernatant for T cell development, as previously described (Carotta et al., 2011). The cells were passaged into a larger well, as necessary, on a new OP9-DL1 layer, when they had achieved maximum confluency. The concentration of SCF was lowered to 50 ng/ml on day 10, and subsequently to 25 ng/ml on day 14 to promote T cell differentiation. Cells were harvested for FACS sorting on day 18. Cells were stained with the fluorescently conjugated antibodies as mentioned above, and sorted on a FACSAria II for DN (double-negative, CD3/$TCR^-CD4^-CD8^-$), DN1 (c-KIT^+ $CD25^-$), and DN2+3 ($CD25^+$) fractions. OP9-DL1 cells were excluded in the sort by their GFP fluorescence.

Western blotting

In vitro–differentiated T cell samples were prepared from 150,000 sorted cells. Tumor samples were prepared from cryopreserved single-cell suspensions. In both cases, lysates were prepared using RIPA buffer with Complete Ultra Protease Inhibitors (Roche).

Protein lysates, loaded at equal quantity, were separated on a NuPAGE Novex 10% Bis-Tris Protein Gel (Thermo Fisher Scientific), followed by iBlot transfer to nitrocellulose (P3 program, 7 min; Thermo Fisher Scientific). Membranes were blocked in 5% skim milk powder in PBS with 0.1% Tween-20, and then probed with the following antibodies, as indicated in the figure legends: polyclonal rabbit anti-BIM (ADI-AAP-330-E; Enzo Life Sciences), rabbit polyclonal anti-p19ARF (Ab80; Abcam), polyclonal rabbit anti-p53 (NCL-p53-CM5p; Leica Biosystems), and monoclonal mouse anti-actin (#A2228, clone AC-74: Sigma-Aldrich), followed by goat anti–rabbit IgG antibodies conjugated to HRP or

goat anti–mouse IgG antibodies conjugated to HRP, respectively (both from Southern Biotech). Blots were developed using the ChemiDoc Touch Imaging System and quantitated with Image Lab Software (both from Bio-Rad Laboratories).

Flow cytometric analysis

Lymphoma phenotype was determined by flow cytometric analysis after staining for hematopoietic subset-specific cell surface markers (B220 [RA3-6B2; WEHI], CD4 [YTA3.2.1; WEHI], CD8 [YTS169; WEHI], IgM [5.1; WEHI], IgD [11-26C; WEHI], TCRβ [H57.59.1; WEHI], Ly5.1 [A20.1; WEHI], and Ly5.2 [5.450.15.2; WEHI]). Staining was performed on ∼10^6 cells for 30 min on ice in the dark. Before analysis, samples were resuspended in medium with propidium iodide (PI, 2 µg/ml; Sigma-Aldrich) and cells were analyzed using a FACSCalibur flow cytometer (BD). Dead cells (PI^+) were excluded from analysis.

Intracellular staining for BIM was performed on isolated thymocytes that had been fixed using the eBioscience Foxp3/Transcription Factor Staining Buffer Set (eBioscience). Surface staining for lineage markers (B220 [RA3-6B2; WEHI] or CD19 [1D3; WEHI], CD4 [YTA3.2.1; WEHI], CD8 [YTS169; WEHI], Gr-1 [RB6-8C5; WEHI], MAC-1 [MI/70; WEHI], Ter119 [TER-119; WEHI], NK1.1 [PK136; WEHI], CD3 [KT3-1; WEHI], and MHC Class II [M5/114; WEHI], as well as CD25 [PC61; WEHI] and CD44 [IM781; WEHI]) was performed. Cells were then fixed in Fix/Perm buffer for 30 min on ice and, afterward, washed with Perm/Wash buffer. The cells were then stained using the 3C5 anti-BIM antibody conjugated to Alexa Fluor 647 (Life Technologies) for 30 min. Cells were washed and analyzed using a LSR-II flow cytometer (BD). DN3 cells were defined as $Lin^-CD25^+CD44^-$. Specific BIM signal was determined relative to a *Bim*$^{-/-}$ sample (negative control).

Statistical analysis

In all cases, sample and mouse numbers were chosen based on previous experience with mice deficient for various BCL-2 family members. All data points were included in final analysis, without exclusions. All animal survival experiments were conducted in a blinded manner with sick mice identified by an experienced mouse technician blinded to their genotype and the hypothesis. Kaplan-Meier animal survival curves were prepared using Prism 6 (GraphPad Software) and statistical comparisons were performed in a pairwise manner using the log-rank (Mantel-Cox) test; $P < 0.05$ was deemed to be statistically significant. Organ weights and blood counts of tumor-bearing mice were plotted using Prism 6 and comparisons were made using the Student's *t* test (unpaired, two-tailed).

ACKNOWLEDGMENTS

We thank all members of the Strasser, Gray, and Herold laboratories for their support and advice, and Dr. P. Fedele for advice and expertise with plasmacytoma analysis. We thank Drs. T. Jacks, A. Villunger, J. Adams, S. Cory, L. Corcoran, C. Scott, and P. Bouillet for gifts of mice; K. Humphries, K. Walker, E. Lanera, J. Mansheim, G. Siciliano, S. O'Connor, K. Trueman, G. Dabrowski, K. Vella, and K. McKenzie for expert animal care; B. Helbert, H. Ierino, K. Mackwell, and C. Young for genotyping; J. Corbin and J. McManus for automated blood analysis; and D. Quilici and T. Nikolaou for γ-radiation services.

This work was supported by grants and fellowships from the Cancer Council of Victoria (S. Grabow and A.R.D. Delbridge [Sydney Parker Smith Postdoctoral Research Fellowship]), Leukemia Foundation National Research Program Clinical PhD Scholarship (B.J. Aubrey), Lady Tata Postdoctoral Fellowship (S. Grabow), the National Health and Medical Research Council (Program grant #1016701; SPRF Fellowship 1020363, A. Strasser; Project Grant #APP1049720, M.J. Herold), the Leukemia and Lymphoma Society (SCOR grant #7001-13), the estate of Anthony (Toni) Redstone OAM, Melbourne International Research Scholarship (University of Melbourne, S. Grabow), Melbourne International Fee Remission Scholarship (University of Melbourne, S. Grabow), Australian Postgraduate Award (A.R.D. Delbridge), Cancer Therapeutics CRC Top-up Scholarship (S. Grabow and ARDD), and the Ian Potter Foundation. This work was made possible by operational infrastructure grants through the Australian Government Independent Medical Research Institutes Infrastructure Support Scheme and the Victorian State Government Operational Infrastructure Support Program.

The authors declare no competing financial interests.

Author contributions: Study and experiments were designed and conceived by A.R.D. Delbridge and A. Strasser. Experiments were conducted and analyzed by all authors. Manuscript was prepared by A.R.D. Delbridge and A. Strasser, with assistance from the other authors.

Submitted: 16 March 2015
Accepted: 8 August 2016

REFERENCES

Alt, F.W., Y. Zhang, F.L. Meng, C. Guo, and B. Schwer. 2013. Mechanisms of programmed DNA lesions and genomic instability in the immune system. *Cell.* 152:417–429. http://dx.doi.org/10.1016/j.cell.2013.01.007

Aubrey, B.J., G.L. Kelly, A.J. Kueh, M.S. Brennan, L. O'Connor, L. Milla, S. Wilcox, L. Tai, A. Strasser, and M.J. Herold. 2015. An inducible lentiviral guide RNA platform enables the identification of tumor-essential genes and tumor-promoting mutations in vivo. *Cell Reports.* 10:1422–1432. http://dx.doi.org/10.1016/j.celrep.2015.02.002

Bouillet, P., D. Metcalf, D.C.S. Huang, D.M. Tarlinton, T.W.H. Kay, F. Köntgen, J.M. Adams, and A. Strasser. 1999. Proapoptotic Bcl-2 relative Bim required for certain apoptotic responses, leukocyte homeostasis, and to preclude autoimmunity. *Science.* 286:1735–1738. http://dx.doi.org/10.1126/science.286.5445.1735

Brady, C.A., D. Jiang, S.S. Mello, T.M. Johnson, L.A. Jarvis, M.M. Kozak, D. Kenzelmann Broz, S. Basak, E.J. Park, M.E. McLaughlin, et al. 2011. Distinct p53 transcriptional programs dictate acute DNA-damage responses and tumor suppression. *Cell.* 145:571–583. http://dx.doi.org/10.1016/j.cell.2011.03.035

Carotta, S., S.H. Pang, S.L. Nutt, and G.T. Belz. 2011. Identification of the earliest NK-cell precursor in the mouse BM. *Blood.* 117:5449–5452. http://dx.doi.org/10.1182/blood-2010-11-318956

Clybouw, C., D. Merino, T. Nebl, F. Masson, M. Robati, L. O'Reilly, A. Hübner, R.J. Davis, A. Strasser, and P. Bouillet. 2012. Alternative splicing of Bim and Erk-mediated Bim(EL) phosphorylation are dispensable for hematopoietic homeostasis in vivo. *Cell Death Differ.* 19:1060–1068. http://dx.doi.org/10.1038/cdd.2011.198

Czabotar, P.E., G. Lessene, A. Strasser, and J.M. Adams. 2014. Control of apoptosis by the BCL-2 protein family: implications for physiology and therapy. *Nat. Rev. Mol. Cell Biol.* 15:49–63. http://dx.doi.org/10.1038/nrm3722

Davidson, W.F., T. Giese, and T.N. Fredrickson. 1998. Spontaneous development of plasmacytoid tumors in mice with defective Fas-Fas ligand interactions. *J. Exp. Med.* 187:1825–1838. http://dx.doi.org/10.1084/jem.187.11.1825

Delbridge, A.R., and A. Strasser. 2015. The BCL-2 protein family, BH3-mimetics and cancer therapy. *Cell Death Differ.* 22:1071–1080. http://dx.doi.org/10.1038/cdd.2015.50

Delbridge, A.R., L.J. Valente, and A. Strasser. 2012. The role of the apoptotic machinery in tumor suppression. *Cold Spring Harb. Perspect. Biol.* 4:12. http://dx.doi.org/10.1101/cshperspect.a008789

Dijkers, P.F., R.H. Medema, J.W. Lammers, L. Koenderman, and P.J. Coffer. 2000. Expression of the pro-apoptotic Bcl-2 family member Bim is regulated by the forkhead transcription factor FKHR-L1. *Curr. Biol.* 10:1201–1204. http://dx.doi.org/10.1016/S0960-9822(00)00728-4

Donehower, L.A., M. Harvey, B.L. Slagle, M.J. McArthur, C.A.J. Montgomery Jr., J.S. Butel, and A. Bradley. 1992. Mice deficient for p53 are developmentally normal but susceptible to spontaneous tumours. *Nature.* 356:215–221. http://dx.doi.org/10.1038/356215a0

Egle, A., A.W. Harris, P. Bouillet, and S. Cory. 2004. Bim is a suppressor of Myc-induced mouse B cell leukemia. *Proc. Natl. Acad. Sci. USA.* 101:6164–6169. http://dx.doi.org/10.1073/pnas.0401471101

Eischen, C.M., J.D. Weber, M.F. Roussel, C.J. Sherr, and J.L. Cleveland. 1999. Disruption of the ARF-Mdm2-p53 tumor suppressor pathway in Myc-induced lymphomagenesis. *Genes Dev.* 13:2658–2669. http://dx.doi.org/10.1101/gad.13.20.2658

Erlacher, M., V. Labi, C. Manzl, G. Böck, A. Tzankov, G. Häcker, E. Michalak, A. Strasser, and A. Villunger. 2006. Puma cooperates with Bim, the rate-limiting BH3-only protein in cell death during lymphocyte development, in apoptosis induction. *J. Exp. Med.* 203:2939–2951. http://dx.doi.org/10.1084/jem.20061552

Frank, K.M., N.E. Sharpless, Y. Gao, J.M. Sekiguchi, D.O. Ferguson, C. Zhu, J.P. Manis, J. Horner, R.A. DePinho, and F.W. Alt. 2000. DNA ligase IV deficiency in mice leads to defective neurogenesis and embryonic lethality via the p53 pathway. *Mol. Cell.* 5:993–1002. http://dx.doi.org/10.1016/S1097-2765(00)80264-6

Fugmann, S.D., A.I. Lee, P.E. Shockett, I.J. Villey, and D.G. Schatz. 2000. The RAG proteins and V(D)J recombination: complexes, ends, and transposition. *Annu. Rev. Immunol.* 18:495–527. http://dx.doi.org/10.1146/annurev.immunol.18.1.495

Gao, Y., D.O. Ferguson, W. Xie, J.P. Manis, J. Sekiguchi, K.M. Frank, J. Chaudhuri, J. Horner, R.A. DePinho, and F.W. Alt. 2000. Interplay of p53 and DNA-repair protein XRCC4 in tumorigenesis, genomic stability and development. *Nature.* 404:897–900. http://dx.doi.org/10.1038/35009138

Greenhough, A., C.A. Wallam, D.J. Hicks, M. Moorghen, A.C. Williams, and C. Paraskeva. 2010. The proapoptotic BH3-only protein Bim is downregulated in a subset of colorectal cancers and is repressed by antiapoptotic COX-2/PGE(2) signalling in colorectal adenoma cells. *Oncogene.* 29:3398–3410. http://dx.doi.org/10.1038/onc.2010.94

Hanahan, D., and R.A. Weinberg. 2011. Hallmarks of cancer: the next generation. *Cell.* 144:646–674. http://dx.doi.org/10.1016/j.cell.2011.02.013

Herold, M.J., L. Rohrbeck, M.J. Lang, R. Grumont, S. Gerondakis, L. Tai, P. Bouillet, T. Kaufmann, and A. Strasser. 2013. Foxo-mediated Bim transcription is dispensable for the apoptosis of hematopoietic cells that is mediated by this BH3-only protein. *EMBO Rep.* 14:992–998. http://dx.doi.org/10.1038/embor.2013.152

Huang, D.C.S., and A. Strasser. 2000. BH3-Only proteins-essential initiators of apoptotic cell death. *Cell.* 103:839–842. http://dx.doi.org/10.1016/S0092-8674(00)00187-2

Jacks, T., L. Remington, B.O. Williams, E.M. Schmitt, S. Halachmi, R.T. Bronson, and R.A. Weinberg. 1994. Tumor spectrum analysis in *p53*-mutant mice. *Curr. Biol.* 4:1–7. http://dx.doi.org/10.1016/S0960-9822(00)00002-6

Jeffers, J.R., E. Parganas, Y. Lee, C. Yang, J. Wang, J. Brennan, K.H. MacLean, J. Han, T. Chittenden, J.N. Ihle, et al. 2003. Puma is an essential mediator of p53-dependent and -independent apoptotic pathways. *Cancer Cell.* 4:321–328. http://dx.doi.org/10.1016/S1535-6108(03)00244-7

Katz, S.G., J.L. Labelle, H. Meng, R.P. Valeriano, J.K. Fisher, H. Sun, S.J. Rodig, S.H. Kleinstein, and L.D. Walensky. 2014. Mantle cell lymphoma in cyclin D1 transgenic mice with Bim-deficient B cells. *Blood.* 123:884–893. http://dx.doi.org/10.1182/blood-2013-04-499079

Kelly, P.N., M.J. White, M.W. Goschnick, K.A. Fairfax, D.M. Tarlinton, S.A. Kinkel, P. Bouillet, J.M. Adams, B.T. Kile, and A. Strasser. 2010. Individual and overlapping roles of BH3-only proteins Bim and Bad in apoptosis of lymphocytes and platelets and in suppression of thymic lymphoma development. *Cell Death Differ.* 17:1655–1664. http://dx.doi.org/10.1038/cdd.2010.43

Kemp, C.J., T. Wheldon, and A. Balmain. 1994. *p53*-deficient mice are extremely susceptible to radiation-induced tumorigenesis. *Nat. Genet.* 8:66–69. http://dx.doi.org/10.1038/ng0994-66

Labi, V., M. Erlacher, S. Kiessling, C. Manzl, A. Frenzel, L. O'Reilly, A. Strasser, and A. Villunger. 2008. Loss of the BH3-only protein Bmf impairs B cell homeostasis and accelerates gamma irradiation-induced thymic lymphoma development. *J. Exp. Med.* 205:641–655. http://dx.doi.org/10.1084/jem.20071658

Ley, R., K.E. Ewings, K. Hadfield, E. Howes, K. Balmanno, and S.J. Cook. 2004. Extracellular signal-regulated kinases 1/2 are serum-stimulated "Bim(EL) kinases" that bind to the BH3-only protein Bim(EL) causing its phosphorylation and turnover. *J. Biol. Chem.* 279:8837–8847. http://dx.doi.org/10.1074/jbc.M311578200

Li, T., N. Kon, L. Jiang, M. Tan, T. Ludwig, Y. Zhao, R. Baer, and W. Gu. 2012. Tumor suppression in the absence of p53-mediated cell-cycle arrest, apoptosis, and senescence. *Cell.* 149:1269–1283. http://dx.doi.org/10.1016/j.cell.2012.04.026

Lord, C.J., and A. Ashworth. 2012. The DNA damage response and cancer therapy. *Nature.* 481:287–294. http://dx.doi.org/10.1038/nature10760

Marculescu, R., T. Le, P. Simon, U. Jaeger, and B. Nadel. 2002. V(D)J-mediated translocations in lymphoid neoplasms: a functional assessment of genomic instability by cryptic sites. *J. Exp. Med.* 195:85–98. http://dx.doi.org/10.1084/jem.20011578

Mestre-Escorihuela, C., F. Rubio-Moscardo, J.A. Richter, R. Siebert, J. Climent, V. Fresquet, E. Beltran, X. Agirre, I. Marugan, M. Marín, et al. 2007. Homozygous deletions localize novel tumor suppressor genes in B-cell lymphomas. *Blood.* 109:271–280. http://dx.doi.org/10.1182/blood-2006-06-026500

Mombaerts, P., J. Iacomini, R.S. Johnson, K. Herrup, S. Tonegawa, and V.E. Papaioannou. 1992. RAG-1-deficient mice have no mature B and T lymphocytes. *Cell.* 68:869–877. http://dx.doi.org/10.1016/0092-8674(92)90030-G

Nakano, K., and K.H. Vousden. 2001. *PUMA*, a novel proapoptotic gene, is induced by p53. *Mol. Cell.* 7:683–694. http://dx.doi.org/10.1016/S1097-2765(01)00214-3

Oda, E., R. Ohki, H. Murasawa, J. Nemoto, T. Shibue, T. Yamashita, T. Tokino, T. Taniguchi, and N. Tanaka. 2000. Noxa, a BH3-only member of the Bcl-2 family and candidate mediator of p53-induced apoptosis. *Science.* 288:1053–1058. http://dx.doi.org/10.1126/science.288.5468.1053

Pellegrini, M., G. Belz, P. Bouillet, and A. Strasser. 2003. Shutdown of an acute T cell immune response to viral infection is mediated by the proapoptotic Bcl-2 homology 3-only protein Bim. *Proc. Natl. Acad. Sci. USA.* 100:14175–14180. http://dx.doi.org/10.1073/pnas.2336198100

Richter-Larrea, J.A., E.F. Robles, V. Fresquet, E. Beltran, A.J. Rullan, X. Agirre, M.J. Calasanz, C. Panizo, J.A. Richter, J.M. Hernandez, et al. 2010. Reversion of epigenetically mediated BIM silencing overcomes chemoresistance in Burkitt lymphoma. *Blood.* 116:2531–2542. http://dx.doi.org/10.1182/blood-2010-02-268003

Strasser, A., A.W. Harris, T. Jacks, and S. Cory. 1994. DNA damage can induce apoptosis in proliferating lymphoid cells via p53-independent

mechanisms inhibitable by Bcl-2. *Cell.* 79:329–339. http://dx.doi.org/10.1016/0092-8674(94)90201-1

Stratton, M.R., P.J. Campbell, and P.A. Futreal. 2009. The cancer genome. *Nature.* 458:719–724. http://dx.doi.org/10.1038/nature07943

Sturm, I., C. Stephan, B. Gillissen, R. Siebert, M. Janz, S. Radetzki, K. Jung, S. Loening, B. Dörken, and P.T. Daniel. 2006. Loss of the tissue-specific proapoptotic BH3-only protein Nbk/Bik is a unifying feature of renal cell carcinoma. *Cell Death Differ.* 13:619–627. http://dx.doi.org/10.1038/sj.cdd.4401782

Tagawa, H., S. Karnan, R. Suzuki, K. Matsuo, X. Zhang, A. Ota, Y. Morishima, S. Nakamura, and M. Seto. 2005. Genome-wide array-based CGH for mantle cell lymphoma: identification of homozygous deletions of the proapoptotic gene BIM. *Oncogene.* 24:1348–1358. http://dx.doi.org/10.1038/sj.onc.1208300

Valente, L.J., D.H. Gray, E.M. Michalak, J. Pinon-Hofbauer, A. Egle, C.L. Scott, A. Janic, and A. Strasser. 2013. p53 efficiently suppresses tumor development in the complete absence of its cell-cycle inhibitory and proapoptotic effectors p21, Puma, and Noxa. *Cell Reports.* 3:1339–1345. http://dx.doi.org/10.1016/j.celrep.2013.04.012

Venkatachalam, S., Y.P. Shi, S.N. Jones, H. Vogel, A. Bradley, D. Pinkel, and L.A. Donehower. 1998. Retention of wild-type p53 in tumors from p53 heterozygous mice: reduction of p53 dosage can promote cancer formation. *EMBO J.* 17:4657–4667. http://dx.doi.org/10.1093/emboj/17.16.4657

Villunger, A., E.M. Michalak, L. Coultas, F. Müllauer, G. Böck, M.J. Ausserlechner, J.M. Adams, and A. Strasser. 2003. p53- and drug-induced apoptotic responses mediated by BH3-only proteins puma and noxa. *Science.* 302:1036–1038. http://dx.doi.org/10.1126/science.1090072

Yu, J., Z. Wang, K.W. Kinzler, B. Vogelstein, and L. Zhang. 2003. PUMA mediates the apoptotic response to p53 in colorectal cancer cells. *Proc. Natl. Acad. Sci. USA.* 100:1931–1936. http://dx.doi.org/10.1073/pnas.2627984100

Zantl, N., G. Weirich, H. Zall, B.M. Seiffert, S.F. Fischer, S. Kirschnek, C. Hartmann, R.M. Fritsch, B. Gillissen, P.T. Daniel, and G. Häcker. 2007. Frequent loss of expression of the pro-apoptotic protein Bim in renal cell carcinoma: evidence for contribution to apoptosis resistance. *Oncogene.* 26:7038–7048. http://dx.doi.org/10.1038/sj.onc.1210510

Zhang, L., T.L. Reynolds, X. Shan, and S. Desiderio. 2011. Coupling of V(D)J recombination to the cell cycle suppresses genomic instability and lymphoid tumorigenesis. *Immunity.* 34:163–174. http://dx.doi.org/10.1016/j.immuni.2011.02.003